AEM
Journals.ASM.org

Genetics and Physiology of Acetate Metabolism by the Pta-Ack Pathway of *Streptococcus mutans*

Jeong Nam Kim, Sang-Joon Ahn, Robert A. Burne

Department of Oral Biology, College of Dentistry, University of Florida, Gainesville, Florida, USA

In the dental caries pathogen *Streptococcus mutans*, phosphotransacetylase (Pta) catalyzes the conversion of acetyl coenzyme A (acetyl-CoA) to acetyl phosphate (AcP), which can be converted to acetate by acetate kinase (Ack), with the concomitant generation of ATP. A Δ*ackA* mutant displayed enhanced accumulation of AcP under aerobic conditions, whereas little or no AcP was observed in the Δ*pta* or Δ*pta* Δ*ackA* mutant. The Δ*pta* and Δ*pta* Δ*ackA* mutants also had diminished ATP pools compared to the size of the ATP pool for the parental or Δ*ackA* strain. Surprisingly, when exposed to oxidative stress, the Δ*pta* Δ*ackA* strain appeared to regain the capacity to produce AcP, with a concurrent increase in the size of the ATP pool compared to that for the parental strain. The Δ*ackA* and Δ*pta* Δ*ackA* mutants exhibited enhanced (p)ppGpp accumulation, whereas the strain lacking Pta produced less (p)ppGpp than the wild-type strain. The Δ*ackA* and Δ*pta* Δ*ackA* mutants displayed global changes in gene expression, as assessed by microarrays. All strains lacking Pta, which had defects in AcP production under aerobic conditions, were impaired in their abilities to form biofilms when glucose was the growth carbohydrate. Collectively, these data demonstrate the complex regulation of the Pta-Ack pathway and critical roles for these enzymes in processes that appear to be essential for the persistence and pathogenesis of *S. mutans*.

Streptococcus mutans is a facultatively anaerobic, Gram-positive bacterium with fermentative metabolism. Human dental caries is associated with increased proportions of multiple acid-tolerant species in tooth biofilms, but *S. mutans* shows a particularly strong association with the initiation and progression of this common infectious disease (1, 2). The pathogenic potential of *S. mutans* is highly dependent on its ability to form biofilms, to use a variety of carbohydrates to produce organic acids that dissolve tooth mineral, and to tolerate stresses commonly encountered in oral biofilms. In particular, tolerance of a variety of reactive oxygen species (ROS), including superoxide ions and hydrogen peroxide, is considered critical for *S. mutans* to overcome antagonism by oral commensals and host defenses (3, 4).

S. mutans has a partial tricarboxylic acid (TCA) cycle and lacks cytochromes, so the primary route for ATP generation by this organism is through the Embden-Meyerhof-Parnas pathway (4–7). Under anaerobic conditions and with growth in the presence of an excess of a preferred carbohydrate, the pyruvate generated by glycolysis is acted on by lactate dehydrogenase (LDH), which is allosterically activated by fructose-1,6-bisphosphate (F-1,6-BP), to produce lactate and regenerate NAD (4, 8). If carbohydrate is limiting, *S. mutans* produces a pyruvate formate lyase enzyme, which converts pyruvate to acetyl coenzyme A (acetyl-CoA) and formate (Fig. 1). However, the pyruvate formate lyase (PFL) enzyme of *S. mutans* is inactivated by oxygen, so under aerobic conditions and if catabolite repression is alleviated (M. Watts and R. A. Burne, unpublished data), the genes for the pyruvate dehydrogenase (PDH) complex are expressed (9) and PDH can catalyze the conversion of pyruvate to acetyl-CoA and CO_2, with the concomitant reduction of NAD^+ to NADH (5, 6). The *S. mutans* genome also encodes a phosphotransacetylase (Pta) enzyme that can utilize acetyl-CoA to generate acetyl phosphate (AcP). AcP can be converted to acetate by acetate kinase (Ack), encoded by the *ackA* gene, with the phosphate moiety being transferred to ADP to produce ATP (Fig. 1) (10). In many organisms, the Pta-Ack pathway is reversible, so cells provided with exogenous acetate can generate acetyl-CoA for anabolic and bioenergetic processes.

AcP has been demonstrated to function as a signaling molecule and to be capable of serving as a phosphate donor for two-component signal transduction systems (TCSs), thereby connecting central metabolism with environmental sensing and signal transduction (11–14). Moreover, the importance of AcP in processes that are critical for bacterial virulence and persistence has been demonstrated in certain eubacteria, including *Escherichia coli* (11, 12, 14), *Staphylococcus aureus* (15), *Streptococcus pneumoniae* (16), *Listeria monocytogenes* (17), and *Clostridium acetobutylicum* (18, 19), although not in *S. mutans* or other oral pathogens. Some effects of AcP on the properties of bacteria related to virulence include the finding that inactivation of the Pta-Ack pathway results in biofilm formation that is quantitatively and architecturally distinct from that in the parental strains (14, 16, 20). In *E. coli*, analysis of the transcriptome showed that the expression of about 100 genes is responsive to intracellular AcP levels, many of which encode products involved in bacterial motility or adherence (14). Also, a mutation in either *ackA* or *pta*, yielding strains that were defective in the degradation or production of AcP, respectively, did not affect cell growth (12, 16) but altered the production of

Received 7 April 2015 **Accepted** 12 May 2015

Accepted manuscript posted online 15 May 2015

Citation Kim JN, Ahn S-J, Burne RA. 2015. Genetics and physiology of acetate metabolism by the Pta-Ack pathway of *Streptococcus mutans*. Appl Environ Microbiol 81:5015–5025. doi:10.1128/AEM.01160-15.

Editor: M. Kivisaar

Address correspondence to Robert A. Burne, rburne@dental.ufl.edu.

Supplemental material for this article may be found at http://dx.doi.org/10.1128/AEM.01160-15.

Copyright © 2015, American Society for Microbiology. All Rights Reserved.

doi:10.1128/AEM.01160-15

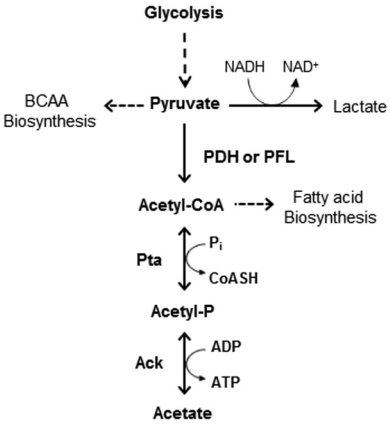

FIG 1 Schematic of the Pta-Ack pathway that produces an AcP from acetyl-CoA and then acetate and ATP. BCAA, branched-chain amino acids; PDH, pyruvate dehydrogenase; PFL, pyruvate formate lyase; P_i, inorganic phosphate; CoASH, coenzyme A.

type 1 pili and flagella, which in turn influenced the initial stages of biofilm development (14). A recent study with *S. aureus* revealed that disruption of the Pta-Ack pathway resulted in growth inhibition, accompanied by a redirection of the carbon flow into multiple metabolic pathways. Notably, there were also changes in the levels of key metabolites, including ATP, NAD^+, NADH, and pyruvate (15). Also of interest, loss of the Pta-Ack pathway in *S. aureus* induced the downregulation of the CidR-regulated *alsSD* and *cidABC* operons, which carry genes involved in the control of cell death associated with a metabolic block at the pyruvate node (15).

In this study, we provide evidence that the Pta-Ack pathway of *S. mutans* is capable of producing intracellular AcP and that the sizes of the AcP pools can be correlated with the abilities of this organism to tolerate oxidative stress and to form biofilms. Our previous investigation demonstrated that the *pta* gene is transcribed as part of the four-gene *relQ* operon, with RelQ being a small (p)ppGpp synthase (21). Other genes in the *relQ* operon include an NAD kinase and pseudouridine synthase, which potentially link acetate (Pta) and (p)ppGpp (RelQ) metabolism with pathways that rely on NADP as a cofactor and with translational efficiency via pseudouridylation of rRNAs, respectively. Of interest, our findings presented here show that inactivation of the Pta-Ack pathway significantly affects (p)ppGpp accumulation in response to oxidative stress, revealing an intimate metabolic linkage between acetate metabolism and (p)ppGpp accumulation (21). This work represents the first comprehensive analysis of the roles of AcP in *S. mutans* and provides new insights into the Pta-Ack pathway and its integration with carbon metabolism and the stringent response.

MATERIALS AND METHODS

Bacterial strains and growth conditions. The strains and plasmids used in this study are listed in Table 1. *Escherichia coli* strains were grown using Luria medium, and *Streptococcus mutans* UA159 and its derivatives were grown using brain heart infusion (BHI) medium (Difco Laboratories, Detroit, MI). The growth media were supplemented with spectinomycin (50 μg/ml for *E. coli* or 1 mg/ml for *S. mutans*), erythromycin (300 μg/ml for *E. coli* or 10 μg/ml for *S. mutans*), or kanamycin (50 μg/ml for *E. coli* or 1 mg/ml for *S. mutans*) (Sigma-Aldrich, St. Louis, MO), when needed. Bacterial growth was measured in the chemically defined medium FMC supplemented with 25 mM glucose as the carbohydrate source, as previously described (22). Briefly, overnight cultures in BHI broth were diluted 1:50 into fresh BHI broth and grown to mid-exponential phase (optical density at 600 nm [OD_{600}] = 0.5) at 37°C in a 5% CO_2 aerobic atmosphere. Mid-exponential-phase cultures were then diluted 1:100 into fresh FMC medium. The optical density at 600 nm of cells growing at 37°C was measured every 30 min using a Bioscreen C lab system (Helsinki, Finland). Sterile mineral oil was overlaid on the cultures to create a less aerobic environment. For oxidative stress conditions, the growth medium was supplemented with 0.003% H_2O_2.

Strain construction. A variety of deletion mutants of *S. mutans* was constructed as described in detail elsewhere (23, 24). Briefly, fragments flanking the gene of interest were amplified with gene-specific primers carrying a BamHI recognition site. The PCR products were digested with BamHI (New England BioLabs) and ligated with T4 DNA ligase (Invitrogen) to a nonpolar kanamycin resistance gene (NPKm) (25) that had been digested with the same restriction enzyme. The resulting ligation mixtures were transformed into competent *S. mutans* cells to allow homologous recombination and allelic replacement. The transformants were isolated on BHI agar plates supplemented with kanamycin. Confirmation that the correct mutation was introduced and that the sequences of the genes used for homologous recombination were not altered was obtained by PCR and DNA sequencing of the PCR products.

Complementation of the *ackA* mutation. A 1,492-bp fragment including the *ackA* gene and its promoter region (26) was PCR amplified using primers *ackA*-BamHI-FW and *ackA*-SphI-RV (Table 2). Following purification of the PCR products, the DNA fragments were digested with BamHI and SphI and cloned into the shuttle vector pDL278 (27) that had been digested with the same restriction enzymes. The recombinant plasmid carrying the *ackA* gene was introduced into the Δ*ackA* strain by competent transformation.

Detection of AcP. Detection of AcP was performed as previously described (28). Briefly, overnight cultures were diluted 1:50 in FMC medium containing 25 mM glucose and grown at 37°C to an OD_{600} of 0.4. One milliliter of each culture was then incubated with 30 μCi [^{32}P]orthophosphate for an additional hour. A 200-μl aliquot of the labeled cells was centrifuged at 10,000 × *g* for 5 min and resuspended in 10 μl of fresh FMC medium. To extract labeled AcP, 10 μl of ice-cold 13 M

TABLE 1 Bacterial strains and plasmids used in this study[a]

Strain or plasmid	Genotype or relevant characteristic(s)	Source or reference(s)
Streptococcus mutans strains		
UA159	Wild type	Laboratory stock
Δ*ackA*	Δ*ackA*::NPKm^r	This study
Δ*pta*	Δ*pta*::NPKm^r	21
Δpta_E	Δ*pta*::NPErm^r	21
Δpta_E Δ*ackA*	Δ*pta* Δ*ackA*::NPKm^r Erm^r	This study
Δ*relA*	Δ*relA*::NPErm^r	31
Δ*relP*	Δ*relP*::NPKm^r	31
Δ*relQ*	Δ*relQ*::NPKm^r	31
Δ*relRS*	Δ*relRS*::NPErm^r	31
KB12	Δ*pta*::NPKm^r carrying pKB101	21
KB034	Δ*ackA*::NPKm^r carrying pKB019	This study
Plasmids		
pDL278	*E. coli-Streptococcus* shuttle vector, Sp^r	38, 55
pKB101	*pta* coding region plus promoter region cloned into pDL278	21
pKB019	*ackA* coding region plus promoter region cloned into pDL278	This study

[a] The integration vector pJL84 is described elsewhere (43).

TABLE 2 Oligonucleotides used in this study

Name	Sequence	Description
ackA-A	TGGGGATTGAGGTTGACGAT	*ackA* deletion
ackA-BamHI-B	ATTTAAGGCGGATCCAACCTGCATT	*ackA* deletion
ackA-BamHI-C	ATGTCGAGCGGATCCAAACTAAATA	*ackA* deletion
ackA-D	TCTGCATCATTGTCCTCCAAGA	*ackA* deletion
ackA-BamHI-FW	TGTCTTAAAGGATCCATCGCAACAA	Complementation
ackA-SphI-RV	CTATTGTACGCATGCCAGAGCGAAA	Complementation

formic acid (Thermo Fisher Scientific, Inc.) was added to the samples. The mixture was subjected to three freeze-thaw cycles, and the supernatants were collected after centrifugation. For removal of unlabeled [^{32}P]orthophosphate, the formic acid extract was incubated with phosphate precipitation buffer (200 mM sodium tungstate, 200 mM tetraethylammonium-HCl) on ice for 2 min. Labeled compounds were recovered after centrifugation at 10,000 × *g* for 15 min, and the supernatants were neutralized by addition of 8 μl of 50 mM procaine. For two-dimensional (2D) thin-layer chromatography (TLC) analysis, the extracts were separated on a 10- by 10-cm polyethyleneimine (PEI)-cellulose plate (Selecto Scientific, Inc., Suwanee, GA) in the first-dimension buffer (0.52 M LiCl, 1% [vol/vol] glacial acetic acid) for 30 min and air dried. The plates were immersed in methanol for 15 min and allowed to air dry. The plates were then chromatographed for 60 min in the second-dimension buffer (1.0 M ammonium acetate, 0.35 M ammonium chloride, adjusted to pH 3.5 with glacial acetic acid) and air dried. The plates were exposed to X-ray film (Kodak) at −80°C. The signal density of spots corresponding to AcP was analyzed using ImageJ (v1.47) software (http://rsbweb.nih.gov/ij/).

Measurement of ATP. ATP was quantified using a CellTiter-Glo luminescent cell viability assay kit (Promega), as described elsewhere (16, 29, 30). Cells were grown in 5 ml of FMC medium supplemented with 25 mM glucose to an OD_{600} of 0.4, collected by centrifugation at 10,000 × *g* at 4°C for 5 min, and washed twice with 250 μl of cold buffer A (10 mM sodium phosphate [pH 7.5], 10 mM $MgCl_2$, 1 mM EDTA). Cells were resuspended in 250 μl of fresh cold buffer and mechanically disrupted in a Bead Beater-16 cell disrupter (Biospec Products, Inc., Bartlesville, OK) with glass beads (diameter, 0.1 mm) twice at 4°C for 30 s each time. Triplicate 50-μl samples of the cell lysate were each mixed with 50 μl of CellTiter-Glo reagent (Promega) in a Costar cell culture 96-well flat-bottom plate (Corning, Inc.). The mixtures were incubated at room temperature for 10 min, and luminescence was measured using a Synergy 2 multimode microplate reader (BioTek Instruments, Inc., USA).

(p)ppGpp accumulation. Measurements of (p)ppGpp were done as detailed elsewhere (31). Overnight cultures were diluted 1:50 in FMC medium supplemented with 25 mM glucose and grown to an OD_{600} of 0.4. Then, 30 μCi of [^{32}P]orthophosphate was added into 200 μl of the cultures, and the mixtures were incubated for an additional hour. Experimental samples were also supplemented with 0.003% (vol/vol) hydrogen peroxide (H_2O_2) at the same time that the [^{32}P]orthophosphate was added. Control cells consisted of aliquots that were labeled in the same manner, but without the addition of hydrogen peroxide. Cells were harvested and resuspended in 10 μl of fresh FMC medium. Nucleotides were extracted by resuspending the cells in 10 μl of ice-cold 13 M formic acid, followed by three freeze-thaw cycles in a dry ice-ethanol bath. The formic acid extracts were spotted directly onto 20- by 20-cm PEI-cellulose plates (Selecto Scientific, Inc., Suwanee, GA) for separation of the phosphorylated nucleotides by TLC. The plates were chromatographed with 1.5 M KH_2PO_4 (pH 3.5), air dried, and exposed to X-ray film (Kodak) at −80°C.

Microarray experiments. Transcriptome analysis was performed as described elsewhere (32, 33) using *S. mutans* UA159 (v3) slides provided by the Pathogen Functional Genomics Resource Center (PFGRC). Briefly, a wild-type strain and two mutant strains (Δ*ackA* and Δ*pta* Δ*ackA* mutants) were grown to exponential phase (OD_{600} = 0.4) in FMC medium supplemented with 25 mM glucose at 37°C in a 5% CO_2 aerobic atmosphere. RNA was isolated using the RNAprotect Bacteria reagent and an RNeasy minikit (Qiagen) and treated with DNase I (Qiagen). Two micrograms of total RNA was used for cDNA synthesis. The Cy5-labeled cDNA from each mutant was mixed with the same amount of the Cy3-labeled cDNA from the wild-type strain and used for microarray hybridization in a MAUI hybridization system (BioMicro Systems). Finally, the slides were washed, dried by centrifugation, and scanned on a GenePix 4400A array scanner (Axon Instruments). Array data were collected using TM4 Spotfinder (v3.2.1) software and normalized using the locally weighted scatterplot smoothing (LOWESS) regression algorithm in MIDAS (v2.22) software (http://www.tm4.org/). Statistical analysis was performed using MultiExperiment Viewer (MeV; v4.8; http://www.tm4.org/mev.html) and BRB-ArrayTools (http://linus.nci.nih.gov/BRB-ArrayTools.html), with a *P* value of 0.005 being considered statistically significant.

Microscopic analysis. *S. mutans* biofilms were observed using a Leica DM IRB confocal laser scanning microscope (CLSM; Leica Microsystems, Wetzlar, Germany) with a Yokogawa spinning disk confocal system (Yokogawa Corporation, Newnan, GA), as previously described (34). Briefly, overnight cultures grown in BHI were diluted 1:50 in fresh BHI and grown to an OD_{600} of 0.4 at 37°C in a 5% CO_2 aerobic atmosphere. The cultures were then diluted 1:100 in 8-well Lab-Tek chamber Permanox slides (Nagle Nunc International, Rochester, NY) containing semidefined biofilm medium (BM) (35) supplemented with 20 mM glucose as the carbohydrate source. Following 24 h or 48 h of incubation, each well was washed twice with 400 μl of Tris-buffered saline (TBS; pH 7.5; 25 mM Tris-HCl, 150 mM NaCl, 2.7 mM KCl). To ascertain the viability of the biofilm and planktonic *S. mutans* cells, cells were stained using a LIVE/DEAD BacLight bacterial viability kit (Molecular Probes, Inc., Eugene, OR) as recommended by the supplier. Slides were stained for 15 min in the dark; the green fluorescent stain SYTO 9 stains live bacteria, and the red fluorescent propidium iodide (PI) stains cells with compromised membranes, which are usually dead. Biofilms were optically sectioned using CLSM, and images were obtained using a 60× oil objective. Simulated *x-y-z* three-dimensional images were generated using ImageJ (v1.47) software. All biofilm experiments were repeated three times with three independent cultures.

Microarray data accession number. All microarray data were deposited in the Gene Expression Omnibus (GEO) database under the accession number GSE46835.

RESULTS

Effects of Ack and Pta on AcP and ATP levels. To evaluate the role of Pta and Ack on the production of intracellular AcP and ATP in *S. mutans*, deletion replacement mutations were created in the *ackA* or *pta* gene, or in both genes, using nonpolar antibiotic resistance genes. The integrity of the mutants and the lack of polarity of the deletion replacements were confirmed using a combination of DNA sequencing and real-time quantitative reverse transcription-PCR (qRT-PCR) analysis, respectively (data not shown). We measured the levels of AcP in the various strains using 2D-TLC after labeling of the cells with [^{32}P]orthophosphate (28, 36), as detailed in the Materials and Methods section. To identify the signal corresponding to AcP, ^{32}P-labeled AcP was prepared using

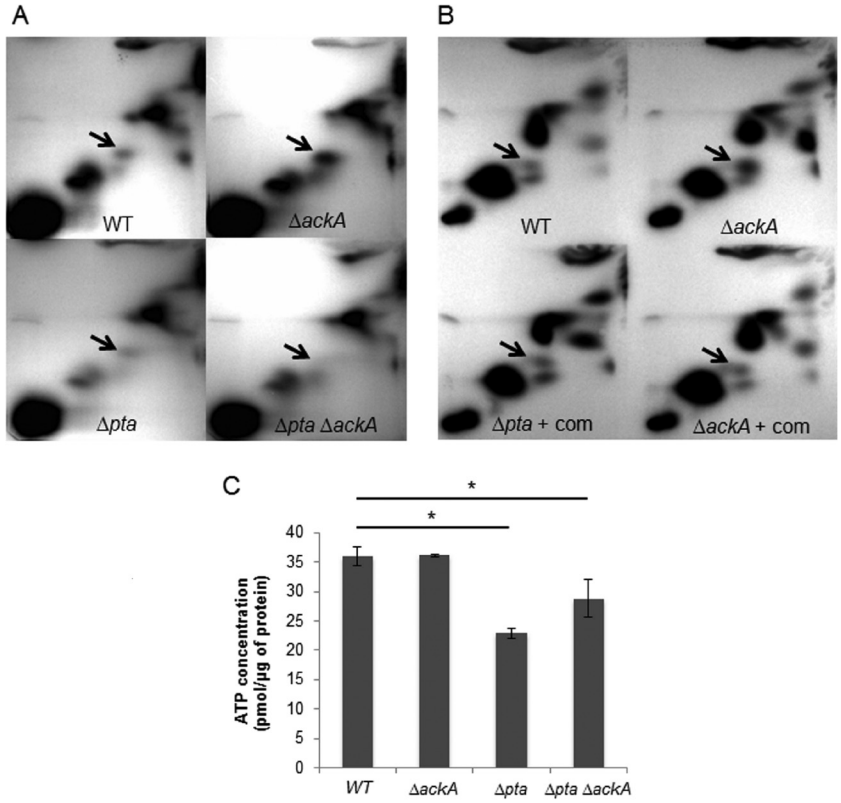

FIG 2 (A) 2D-TLC. AcP levels in acid extracts of cells that were labeled with [^{32}P]orthophosphate were monitored. Arrows, the position to which AcP migrates. Strains include the wild-type (WT) and Δ*ackA*, Δ*pta*, and Δ*pta* Δ*ackA* double mutant strains, as indicated by the labels. (B) Complementation of *ackA* and *pta* mutations. Accumulation of AcP in the wild-type and Δ*ackA* mutant strains compared with that in the Δ*pta* and Δ*ackA* mutants in which the defective gene was complemented with a wild-type copy of *pta* (Δ*pta* + com) or *ackA* (Δ*ackA* + com). (C) Measurement of ATP. The wild-type, Δ*ackA*, Δ*pta*, and Δ*pta* Δ*ackA* strains were grown aerobically to early exponential phase in FMC medium, harvested, and resuspended in 250 μl cold buffer A (see details in Materials and Methods). Cells were lysed, and 50 μl of the lysates was reacted with an equal volume of the luminescent reagent. Luminescence intensity was measured using a Synergy 2 multimode microplate reader. The values shown are the means ± standard deviations for cell lysates from three separate cultures. *, the result differs significantly ($P < 0.05$, Student's *t* test) from that obtained in the wild-type genetic background. The results are expressed as means from triplicate assays for three independent isolates.

a procedure described elsewhere (11), and the migration of metabolites in the acid extracts of *S. mutans* was compared with that of *S. mutans* acid extracts that were spiked with the synthetic [^{32}P]AcP standard (see Fig. S1 in the supplemental material). No AcP was detected in the strain lacking both Pta and Ack, whereas the *ackA* deletion mutant displayed an enhanced accumulation of AcP compared to that for all other strains (Fig. 2A; see also Table S1 in the supplemental material), likely due to the fact that the conversion of AcP to acetate was blocked (11, 12, 16). The strain lacking the *pta* gene accumulated lower levels of AcP than the wild-type and *ackA* mutant strains (18). The data obtained with chromatography of labeled cell extracts was confirmed using an enzymatic assay to detect AcP (see Fig. S2 in the supplemental material) (16). Further, to confirm that the changes in AcP accumulation described above resulted directly from the loss of either *ackA* or *pta*, a plasmid-borne copy of the *ackA* or *pta* gene driven from their cognate promoters (pKB019 or pKB101, respectively) was introduced into the *ackA* and *pta* mutants, respectively. Complementation with the individual genes on a plasmid restored the levels of AcP accumulation to those observed in *S. mutans* UA159 (Fig. 2B; see also Table S1 in the supplemental material).

To examine the impact of the Pta-Ack pathway on ATP production, intracellular ATP levels were measured using the luminescence-based assay detailed in the Materials and Methods section (Fig. 2C). When cells were grown aerobically, inactivation of the *ackA* gene had no significant effect on ATP levels (36.1 ± 0.2 pmol/μg protein) compared to the ATP levels found for the parental strain (36.0 ± 1.6 pmol/μg protein). In contrast, the Δ*pta* and Δ*pta* Δ*ackA* strains exhibited reduced ATP pools (22.9 ± 0.8 and 28.8 ± 3.2 pmol/μg protein, respectively). Collectively, these results indicate that the Pta-Ack pathway is critical for AcP production and enhances ATP generation in *S. mutans* under aerobic conditions.

Effects of Pta-Ack pathway on oxidative stress. Oxidative stress tolerance is generally recognized to be essential for the persistence and cariogenic potential of *S. mutans* (9, 37, 38). To assess whether the mutant strains had altered resistance to oxidative stress, the ability of the organisms to grow in the presence of hydrogen peroxide was examined. The strains harboring the Δ*pta* and Δ*pta* Δ*ackA* mutations had significantly longer doubling times (157 min ± 23 min and 159 min ± 22 min, respectively) in cultures supplemented with 0.003% H_2O_2 than the wild-type strain (103 min ± 17 min) ($P < 0.05$) (Fig. 3A). Further, the Δ*ackA* strain (143 min ± 29 min) also grew more slowly than the wild-type strain ($P < 0.05$) but exhibited a higher growth rate than the strains lacking the *pta* gene.

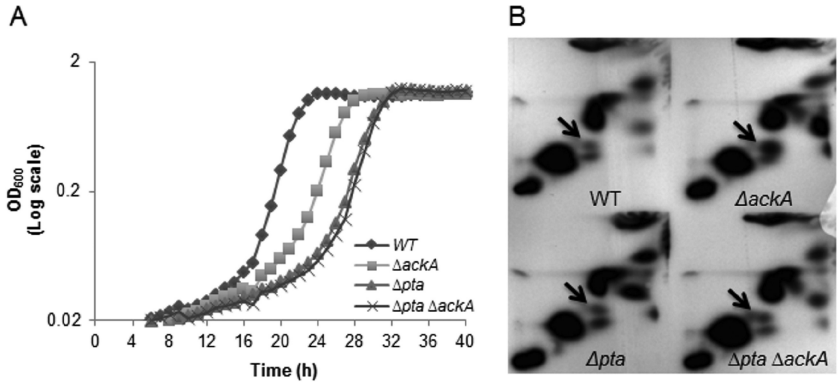

FIG 3 Growth and accumulation of AcP under stress conditions. (A) Growth of the wild-type, Δ*ackA*, Δ*pta*, and Δ*pta* Δ*ackA* strains was monitored in medium supplemented with 0.003% (vol/vol) H_2O_2 under relatively anaerobic conditions (see Materials and Methods for details) at 37°C using a Bioscreen C lab system. Data are expressed as the means of the results for three independent isolates grown in triplicate wells. (B) AcP accumulation of the wild-type, Δ*ackA*, Δ*pta*, and Δ*pta* Δ*ackA* strains was detected when cells were grown in the presence of 0.003% hydrogen peroxide. Cells were grown to the early exponential phase (OD_{600} = 0.4) in FMC medium, and cells were concurrently labeled with [^{32}P]orthophosphate and subjected to the stress conditions for 1 h. AcP and P_i derived from *S. mutans* extracts by formic acid were spotted onto PEI-cellulose plates for 2D-TLC using first-dimension buffer (0.52 M LiCl and 1% [vol/vol] glacial acetic acid) and second-dimension buffer (1 M ammonium acetate and 0.35 M ammonium chloride). Arrows, the spot corresponding to AcP.

To investigate whether intracellular AcP levels fluctuated in response to environmental stress, we monitored via 2D-TLC AcP accumulation in cells grown under the conditions described above. When grown in defined medium supplemented with hydrogen peroxide, the *ackA* deletion mutant exhibited a 2-fold higher level of accumulation of AcP than the wild type and the other mutant strains ($P < 0.05$) (Fig. 3B; see also Table S1 in the supplemental material). In contrast, the strain lacking both genes, surprisingly, exhibited AcP accumulation at levels about 1.2-fold higher than those seen with the wild-type and Δ*pta* mutant strains, albeit the differences were not statistically significant. To demonstrate that the species detected in the double mutant that migrated the same as AcP was indeed AcP, additional experiments were performed. The first was to treat the ^{32}P-labeled mixture with acetate kinase, which resulted in the complete disappearance of the apparent AcP (data not shown). The second was to measure the levels of AcP in cells enzymatically (see Fig. S3 in the supplemental material). While cells that did not produce a spot migrating as AcP in TLC did not show detectable AcP in the biochemical assay, AcP was measured at the expected levels in the double mutant that was treated with H_2O_2. Thus, it must be considered that, under some sets of conditions, *S. mutans* has a mechanism to generate AcP independently of the Pta-Ack pathway.

Inactivation of the Pta-Ack pathway affects (p)ppGpp and ATP levels. Since *pta* is present downstream of and in the same operon as the small (p)ppGpp synthase RelQ (21) and because the double mutant strains had a significantly reduced intracellular concentration of ATP (Fig. 2C), which can be used for (p)ppGpp synthesis, we explored whether there were connections between AcP, ATP production, and (p)ppGpp accumulation in cells that were grown in FMC medium supplemented with or without 0.003% H_2O_2 (39, 40). Accumulation of (p)ppGpp in the Δ*ackA* and Δ*pta* Δ*ackA* strains was significantly greater (~25%) than that in the wild-type strain when cells were labeled in the presence of H_2O_2 (Fig. 4A). However, the Δ*pta* strain exhibited substantially lower levels of (p)ppGpp accumulation than the wild-type strain.

The levels of ATP were measured in cells exposed to hydrogen peroxide. The Δ*ackA* and Δ*pta* Δ*ackA* strains contained more ATP (64.9 ± 1.8 and 88.0 ± 4.2 pmol/μg protein, respectively; $P < 0.05$) and the Δ*pta* strain produced significantly less ATP (37.0 ± 0.8 pmol/μg protein) than the parental strain (57.5 ± 2.6 pmol/μg protein) ($P < 0.05$) (Fig. 4B). Thus, all strains exhibited a positive correlation between (p)ppGpp accumulation and ATP pools under oxidative stress conditions (Fig. 4A and B).

Inactivation of *pta* or both *pta* and *ackA* reduces biofilm formation by *S. mutans*. The ability to form biofilms is believed to be required for *S. mutans* to persist in the human oral cavity. Biofilm formation by the wild-type and mutant strains was assessed by growing cells in a semidefined biofilm medium (BM) supplemented with 20 mM glucose. Images of the biofilms were obtained after 24 and 48 h of incubation using CLSM (Fig. 5), as detailed in the Materials and Methods section. After 24 h of growth, biofilms of the Δ*pta* and Δ*pta* Δ*ackA* mutant strains were sparse and contained little biomass, whereas the wild-type and Δ*ackA* mutant strains formed thick biofilms that covered a greater proportion of the substratum (Fig. 5A). Of interest, both biofilm and planktonic cells lacking *ackA* displayed chains of cells shorter than the chains of cells of the parental strain. After 48 h of incubation, the wild-type strain formed the most robust biofilms in terms of thickness and coverage of the substratum. The strain lacking only *pta* displayed the poorest capacity to form biofilms. Strains lacking *ackA* or both *pta* and *ackA* formed biofilms better than the *pta* single mutant at the 48-h time point but did so nowhere near as efficiently as the wild-type strain (Fig. 5B). Thus, the results support the hypothesis that AcP may function as an important signaling molecule governing the maturation of biofilms by *S. mutans* and that both increases and decreases in AcP pools can influence the biofilm architecture.

Transcription profiling. To identify genes that are potentially responsive to AcP levels, we used microarrays to monitor the transcriptomes of the Δ*ackA* mutant and the Δ*pta* Δ*ackA* mutant, i.e., cells with elevated AcP levels and cells lacking detectable AcP, respectively, and the wild-type strain. When the Δ*ackA* and wild-type strains were compared, 111 genes were differentially expressed ($P < 0.005$), with the expression of 58 genes being upregulated and that of 53 genes being downregulated (Fig. 6A; see also

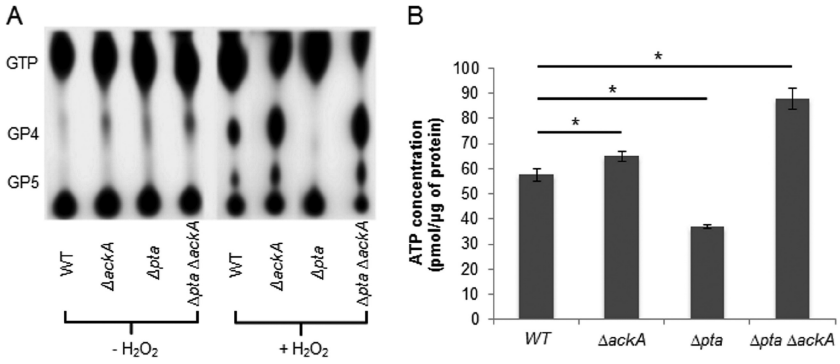

FIG 4 Accumulation of (p)ppGpp and cellular ATP generation under stress conditions. (A) The (p)ppGpp accumulation of the wild-type strain was compared with that of the Δ*ackA*, Δ*pta*, and Δ*pta* Δ*ackA* strains grown in FMC medium supplemented with (+) and without (−) 0.003% hydrogen peroxide. Strains were labeled with [^{32}P]orthophosphate in FMC medium. ^{32}P-labeled nucleotides were extracted by adding an equal volume of 13 M formic acid, followed by three freeze-thaw cycles in a dry ice-ethanol bath. Acid extracts were spotted onto PEI-cellulose plates for TLC in 1.5 M KH_2PO_4 buffer. (B) The amount of ATP in the wild-type strain and the Δ*ackA*, Δ*pta*, and Δ*pta* Δ*ackA* mutants was measured after they were grown to early exponential phase in FMC medium supplemented with and without 0.003% hydrogen peroxide (see details in Materials and Methods). Fifty microliters of cell lysate was reacted with an equal volume of the luminescent reagent. Luminescence intensity was measured using a Synergy 2 multimode microplate reader. Values shown are the means ± standard deviations for cell lysates from three separate cultures. *, the result differs significantly ($P < 0.05$, Student's *t* test) from that for the wild-type genetic background. The results are expressed as means from triplicate assays for three independent isolates.

Table S2 in the supplemental material). Of note, genes encoding products involved in DNA metabolism and cell division and genes for ABC transporters were more highly expressed in the Δ*ackA* mutant than in the parental strain. Conversely, a number of genes encoding products involved in energy metabolism showed a lower level of transcription. Interestingly, the expression of one ortholog of *spxA* (SMU.2084c) that encodes a transcriptional regulator known to positively regulate genes in response to oxidative stress (41) was increased about 1.5-fold, whereas SMU.1548c, encoding a histidine kinase of a TCS, was downregulated approximately 30%. Interestingly, the *ackA* mutant exhibited a 2-fold increase in the level of transcription of *wapA* (SMU.987), encoding a cell wall-associated protein implicated in sucrose-independent aggregation and biofilm formation (42). Previously, a *wapA* mutant of *S. mutans* UA140 was shown to have substantially impaired biofilm formation under low-sucrose conditions (42). These changes in expression of *wapA* and *spx* are thus consistent with the observed alterations in biofilm formation and oxidative stress tolerance, respectively, by the *ackA* mutant.

In the strain lacking *pta* and *ackA*, which exhibits no detectable AcP under aerobic conditions, a total of 92 genes showed altered expression under the conditions tested ($P < 0.005$) (Fig. 6B; see also Table S3 in the supplemental material). The transcription of 32 of these genes was upregulated, while 60 genes, primarily involved in energy metabolism or ABC transporters, including the gene for the LuxS enzyme that produces the proposed signaling molecule autoinducer-2 (AI-2), were significantly downregulated in the Δ*pta* Δ*ackA* mutant compared to their regulation in the parental strain (Fig. 6B). The production of a functional LuxS enzyme and AI-2 has been linked with biofilm maturation and stress tolerance (43), although it is not clear if this is due to quorum sensing or alterations in the activated methyl cycle.

The microarray data were also analyzed in a way that compared gene expression levels in the Δ*ackA* mutant with those in the Δ*pta*

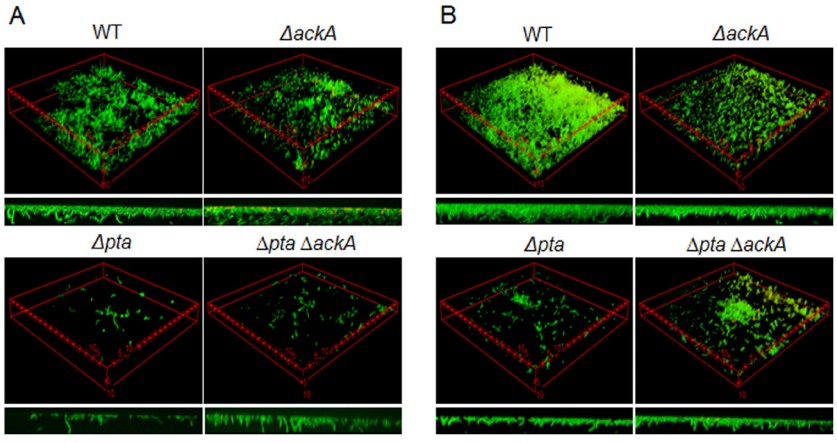

FIG 5 Confocal microscopic images of biofilms. Biofilms of *S. mutans* UA159 and mutant strains were grown in BM supplemented with 20 mM glucose for 24 h (A) or 48 h (B) at 37°C in a 5% CO_2 atmosphere. The data presented are representative of those from three independent experiments. The distance between two asterisks is 5 μm per side. Small images at the bottom present biofilm thickness. See the Materials and Methods section for details on labeling and image analysis.

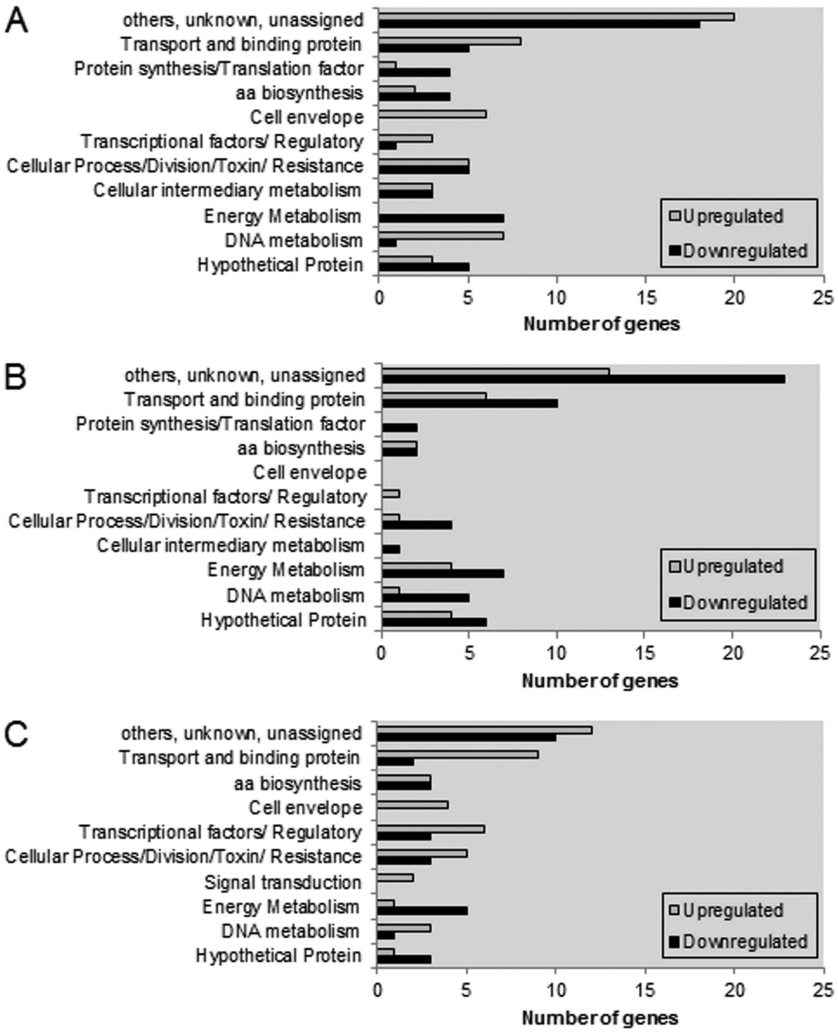

FIG 6 Numbers of genes grouped by functional categories that were differently expressed between wild-type and Δ*ackA* strains (A), between wild-type and Δ*pta* Δ*ackA* strains (B), and between Δ*ackA* and Δ*pta* Δ*ackA* strains (C). Gene annotations are based on information provided by the Los Alamos National Laboratory (http://www.oralgen.org). aa, amino acid.

Δ*ackA* mutant. Using this analysis, 76 genes were distinctly regulated between the two mutants ($P < 0.005$) (Fig. 6C; see also Table S4 in the supplemental material). The transcription of 46 genes, primarily ABC transporters, transcription factors, and cell division, was upregulated in the Δ*ackA* mutant, which had high levels of AcP compared to the levels in the Δ*pta* Δ*ackA* mutant, whereas the transcription of 30 genes was downregulated, with the most significant functional category being energy metabolism (*mmuM*, *adhB*, *adhC*, *citZ*, *cilB*) (see Table S4 in the supplemental material). Significant upregulation of the expression of the *wapA* and *spxA* genes in the Δ*ackA* mutant compared to their expression in the double mutant was observed. Taken together, the results of our transcription profiling support the argument that AcP levels have major effects, probably both directly and indirectly, on the expression of genes that are required for biofilm development and that could affect the persistence and pathogenic potential of *S. mutans*.

DISCUSSION

Cells in the oral cavity experience prolonged periods of carbohydrate limitation during fasting periods but are repeatedly exposed throughout the day to conditions where carbohydrates are transiently present in excess from the dietary intake of foodstuffs. Redox and exposure to oxygen also vary considerably as a function of the maturity of biofilms and sites in the oral cavity (3). Growth of *S. mutans* under aerobic conditions demands a substantial amount of energy to regenerate the NADH that is utilized by NADH oxidase enzymes as a primary defense against damage from reactive oxygen species (ROS) (3, 44). NAD can be phosphorylated to NADP(H) by NAD^+ kinase and ATP, and the *S. mutans* genome encodes a small number of NADP-dependent enzymes that, like NAD/NADH, function in multiple redox reactions. In addition to effects on substrates for redox reactions, aerobic growth results in a shift in the flow of pyruvate away from the oxygen-sensitive PFL enzyme to the PDH complex, allowing the production of an additional ATP through the Pta-Ack pathway. Despite the recognition that successful competition of *S. mutans* with commensal bacteria occurs under conditions where the carbohydrate source and availability are in constant flux and that oxidative stress tolerance is essential for *S. mutans* to cope with the antagonistic strategies of beneficial organisms, the Pta-Ack path-

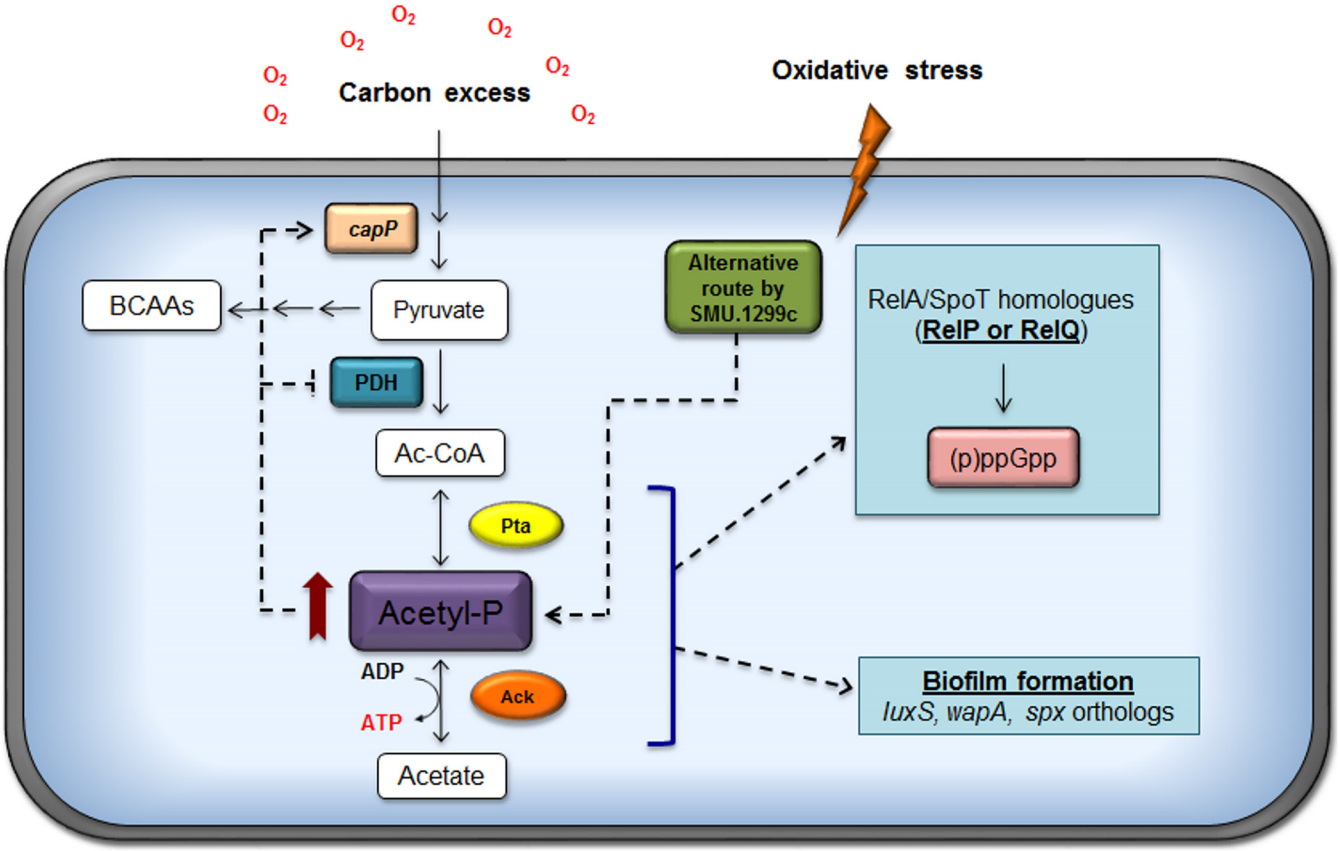

FIG 7 Current model for the role of the Pta-Ack pathway in *S. mutans*. The activities of products encoded by the *ackA* or *pta* genes are primarily responsible for the generation of AcP, the levels of which strongly influence physiology and gene expression in *S. mutans*. In particular, the role of the Pta-Ack pathway in modulating the expression of genes involved in carbohydrate flux at the pyruvate node, as well as those contributing to biofilm formation and stress tolerance, is significant. Moreover, a metabolic linkage between acetate metabolism and (p)ppGpp production in response to oxidative stress is established and is probably mediated by the small (p)ppGpp synthase RelP and the two-component signal transduction system RelRS. Red arrow, high level of accumulation of AcP; dashed arrows, the observations and models.

way has not been studied in any detail in *S. mutans* or other oral streptococci. The results presented here provide novel and significant insights into how control of the Pta-Ack pathway is integrated with oxidative stress responses and biofilm formation in *S. mutans* by coordination of acetate utilization with modulation of (p)ppGpp pools, as summarized in Fig. 7.

Our findings clearly show that the *S. mutans* Pta-Ack pathway is a major contributor to AcP and ATP pools in cells that are aerated. Under aerobic conditions, inactivation of the *S. mutans* Pta-Ack pathway completely blocked AcP generation, indicating that the Pta-Ack pathway is critical for the production of AcP. Moreover, the strain carrying the *pta* mutation grew slightly more slowly than the wild-type and other mutant strains, confirming our previous results (21), whereas mutants lacking either *ackA* alone or both the *pta* and *ackA* genes behaved like the wild-type strain for growth under aerobic conditions (data not shown). These observations are clear evidence for our hypothesis that a sufficient level of ATP via the Pta-Ack pathway needs to be maintained for the normal growth behavior of *S. mutans*.

Hydrogen peroxide is produced in significant quantities by many beneficial commensal streptococci and inhibits the growth of *S. mutans* at physiologically relevant concentrations (45). In contrast, *S. mutans* produces little or no hydrogen peroxide, depending on the growth conditions. In the presence of hydrogen peroxide, the *pta* mutant consistently grew more slowly than the parental strain and displayed significantly decreased ATP pools. Unlike the *pta* mutant, the Δ*ackA* and Δ*pta* Δ*ackA* mutants had ATP levels that were at least as high as those of the parental strain (Fig. 4B), but these strains still displayed substantial growth inhibition in the presence of hydrogen peroxide (Fig. 3A). Thus, rather than a shortage of ATP, the observed growth inhibition of these mutant strains could be due to metabolic toxicity arising from abnormal levels of metabolites, such as AcP, pyruvate, or acetyl-CoA (15, 17). Deletion of the *ackA* gene of *S. aureus* resulted in a growth defect but also resulted in increases in the amounts of AcP, pyruvate, and acetyl-CoA (15). Therefore, we hypothesize that the accumulation of higher levels of AcP in the *ackA* single deletion strain or the *pta* and *ackA* double deletion strain may inhibit the expression or activity of the PDH complex under the conditions tested, leading to an increase in intracellular pyruvate levels, similar to the findings for *S. aureus* (15, 39). Indeed, our transcriptome analysis revealed that an *ackA* mutation and the elevation in AcP pools were associated with reduced transcription of the *pdhA* and *pfl-2* genes that encode pyruvate dehydrogenase (E1 alpha subunit) and formate acetyltransferase, respectively (see Table S2 in the supplemental material). In other words, accumu-

lation of AcP seems to prevent the interconversion of pyruvate to acetyl-CoA, possibly causing a metabolic block at the pyruvate–acetyl-CoA node in the cells. On the other hand, the *capP* gene, which encodes a phosphoenolpyruvate (PEP) carboxylase that is allosterically activated by acetyl-CoA and fructose-1,6-bisphosphate (F-1,6-BP) (46–48), is upregulated in the *ackA* deletion strain. Therefore, the observation of increased AcP and ATP levels coupled with the changes at the transcriptional levels supports the idea that inactivation of the Pta-Ack pathway may cause certain metabolites to accumulate to growth-inhibitory levels, leading to a decreased capacity of *S. mutans* to cope with ROS.

An unexpected result of this study is the finding that AcP appears to be produced in cells lacking an intact Pta-Ack pathway, but only when the mutants were exposed to hydrogen peroxide. Evidence supporting the suggestion that AcP was indeed produced under these conditions included TLC of labeled cell extracts and enzymatic assays showing ATP generation from the cell lysates in the presence of highly purified acetate kinase. One alternative route for AcP generation that is present in a number of Gram-positive cocci with low G+C contents, including some oral streptococci, is xylulose 5-phosphate (X5P)/fructose 6-phosphate (F6P) phosphoketolase (Xfp) (49). The Xfp enzyme catalyzes the conversion of F6P, in the presence of inorganic phosphate, to erythrose 4-phosphate and AcP. Apparent homologs of the gene for Xfp can be found in *Streptococcus gordonii*, *Streptococcus agalactiae*, and a number of lactococci and lactobacilli, but the gene is absent in *S. mutans* UA159. In *S. pneumoniae*, pyruvate oxidase (SpxB) is capable of directly converting pyruvate to AcP when cells are grown aerobically, and the introduction of a deletion of either *pta* alone or both *pta* and *ackA* into the *spxB* mutant background caused AcP levels to drop to negligible amounts (16). However, there is no gene for an apparent *spxB* homologue in *S. mutans*. Thus, we posit that the most likely route for AcP generation in the strain lacking Pta and Ack is through a hypothetical protein with an as-yet-unknown function or via acetate uptake and the subsequent action of the product of the SMU.1299c gene, which is annotated as a putative acetate kinase at http://www.microbesonline.org. In *Lactococcus lactis*, two Ack isozymes (annotated AckA1 and AckA2) are present, and AckA2 has a significantly higher affinity for acetate than AckA1 (50, 51). Although there was no significant similarity between *ackA* and SMU.1299c in nucleotide and amino acid sequences, the biological role of the putative acetate kinase in acetate metabolism must now be considered (Fig. 7). To begin to explore a contribution of SMU.1299c to AcP production in preliminary fashion, we introduced a deletion of SMU.1299c into the *pta ackA* mutant background and measured intracellular AcP levels when the strain was grown in the presence of oxidative stress. Interestingly, the mutant strain had AcP levels that were substantially reduced compared with those of the double mutant but still had higher levels than the wild-type strain (data not shown). Future studies will probe in more detail these potential compensatory or conditional routes of AcP production.

Several observations support the suggestion that the Pta-Ack pathway has a profound effect on (p)ppGpp metabolism in response to oxidative stress. An important observation was the positive correlation among AcP, ATP, and (p)ppGpp pools during oxidative stress. Previously, our laboratory revealed that oxidative stress leads to (p)ppGpp accumulation in the wild-type, Δ*relA*, and Δ*relQ* strains (21). In contrast, a strain lacking RelP or the RelRS two TCS, which was shown to positively regulate *relP*, had lower levels of (p)ppGpp than the aforementioned strains (see Fig. S4 in the supplemental material) (52). Thus, as a part of our working model, we hypothesize that the higher levels of AcP and ATP associated with the disruption of the Pta-Ack pathway have a positive impact on the RelP-dependent production of (p)ppGpp (Fig. 7). The model could accommodate the findings that the *pta* and *ackA* mutant strains, which exhibit higher levels of both AcP and ATP, showed an enhanced accumulation of (p)ppGpp under oxidative stress conditions where the apparent alterative pathway for AcP generation is activated (Fig. 3B and 4A). Moreover, the Δ*pta* Δ*ackA* double mutant showed remarkably enhanced promoter activity and transcription of the *relP* gene when cells were grown under the same conditions (unpublished results). That is, the overproduction of AcP and ATP in the *ackA* and *pta ackA* mutant strains in response to elevated reactive oxygen species could somehow lead to an increase in RelP-dependent (p)ppGpp production, which results in the slower growth of the cells. Notwithstanding, the possibility that RelQ contributes to (p)ppGpp pools cannot be excluded from consideration, because the *pta* gene can be cotranscribed with *relQ*, implying a functional interrelationship between the gene products. It is also notable that PpnK (Nad kinase) and RluE (pseudouridylation of rRNA), which affect oxidation-reduction reactions and translational efficiency and fidelity, respectively, are also encoded in the *relQ* operon (21).

Our transcriptional profiling has helped to identify genes that are regulated in response to AcP levels and has revealed that the status of AcP pools could affect the expression of genes involved in biofilm formation and carbon metabolism (see Tables S2 to S4 in the supplemental material). Specifically, we found that the transcription of two genes (*spxA* and *wapA*) was enhanced in the *ackA* mutant strain, while transcription of the *luxS* gene was reduced in the *pta ackA* mutant, where no AcP was detected under the conditions tested. The microarray results were confirmed using real-time qRT-PCR (see Fig. S5 in the supplemental material). The observation that disruption of the Pta-Ack pathway reduced the ability of *S. mutans* to form biofilms is similar to what was noted for *L. monocytogenes* (17). Previous studies have demonstrated that the *luxS* and *wapA* genes are required for efficient biofilm formation by *S. mutans* strains (42, 43, 53). In contrast, Pamp et al. revealed that inactivation of *spx* enhances biofilm formation by *S. aureus* (54). Of note, the Spx protein is highly conserved between *S. aureus* and *S. mutans*, with 59% identity and 79% homology, and they also have a conserved N-terminal CXXC motif. The inverse relationship of the transcription of *spxA* and the efficiency of biofilm formation by *S. mutans* may reflect the fact that AcP and other factors simply play a more dominant role than SpxA in biofilm maturation in *S. mutans*. Conversely, there are two orthologs (*spxA* and *spxB*) of the Spx transcriptional regulator in the *S. mutans* genome (41), and SpxB may be a more significant contributor to the biofilm phenotype. Notably, SpxB has a minor effect on growth under conditions of oxidative stress but appears to play a significant role in cell wall homeostasis (41), which could have a major impact on cell surface characteristics that mediate biofilm formation or stability. While the relationship of AcP to the Spx regulon needs to be explored in more detail, AcP can clearly affect the production of a spectrum of gene products that impact the physiology and persistence of *S. mutans*.

Concluding remarks. Considering that the Pta-Ack pathway controls the steady-state levels of AcP and ATP and has an impact on stress tolerance, biofilm development, and (p)ppGpp metabo-

lism, our findings provide evidence that that activity of this pathway is critical for *S. mutans*, especially during exposure to elevated levels of oxygen. The Pta-Ack pathway may affect (p)ppGpp metabolism by RelQ and/or RelP when cells experience oxidative stress so as to moderate growth rates and alter gene expression in a way that optimizes the capacity of *S. mutans* to cope with ROS that are generated by competing commensals or from endogenous metabolism involving single electron reductions of oxygen. Future studies will be oriented toward examining the molecular mechanisms by which AcP and acetate metabolism are integrated with essential pathways for the persistence and virulence of *S. mutans*.

ACKNOWLEDGMENTS

This work was supported by National Institute of Dental and Craniofacial Research grant DE13239 from the NIH/NIDCR.

We thank Sug-Joon Ahn and Scott Grieshaber for technical support with confocal microscopy.

REFERENCES

1. **Belda-Ferre P, Alcaraz LD, Cabrera-Rubio R, Romero H, Simon-Soro A, Pignatelli M, Mira A.** 2012. The oral metagenome in health and disease. ISME J **6:**46–56. http://dx.doi.org/10.1038/ismej.2011.85.
2. **Takahashi N, Nyvad B.** 2011. The role of bacteria in the caries process: ecological perspectives. J Dent Res **90:**294–303. http://dx.doi.org/10.1177/0022034510379602.
3. **Marquis RE.** 1995. Oxygen metabolism, oxidative stress and acid-base physiology of dental plaque biofilms. J Ind Microbiol **15:**198–207. http://dx.doi.org/10.1007/BF01569826.
4. **Lemos JA, Abranches J, Burne RA.** 2005. Responses of cariogenic streptococci to environmental stresses. Curr Issues Mol Biol **7:**95–107.
5. **Ajdic D, McShan WM, McLaughlin RE, Savic G, Chang J, Carson MB, Primeaux C, Tian R, Kenton S, Jia H, Lin S, Qian Y, Li S, Zhu H, Najar F, Lai H, White J, Roe BA, Ferretti JJ.** 2002. Genome sequence of *Streptococcus mutans* UA159, a cariogenic dental pathogen. Proc Natl Acad Sci U S A **99:**14434–14439. http://dx.doi.org/10.1073/pnas.172501299.
6. **Carlsson J, Kujala U, Edlund MB.** 1985. Pyruvate dehydrogenase activity in *Streptococcus mutans*. Infect Immun **49:**674–678.
7. **Wolfe AJ.** 2005. The acetate switch. Microbiol Mol Biol Rev **69:**12–50. http://dx.doi.org/10.1128/MMBR.69.1.12-50.2005.
8. **Brown AT, Wittenberger CL.** 1972. Fructose-1,6-diphosphate-dependent lactate dehydrogenase from a cariogenic streptococcus: purification and regulatory properties. J Bacteriol **110:**604–615.
9. **Ahn SJ, Wen ZT, Burne RA.** 2007. Effects of oxygen on virulence traits of *Streptococcus mutans*. J Bacteriol **189:**8519–8527. http://dx.doi.org/10.1128/JB.01180-07.
10. **Warner JB, Lolkema JS.** 2003. CcpA-dependent carbon catabolite repression in bacteria. Microbiol Mol Biol Rev **67:**475–490. http://dx.doi.org/10.1128/MMBR.67.4.475-490.2003.
11. **McCleary WR, Stock JB.** 1994. Acetyl phosphate and the activation of two-component response regulators. J Biol Chem **269:**31567–31572.
12. **Klein AH, Shulla A, Reimann SA, Keating DH, Wolfe AJ.** 2007. The intracellular concentration of acetyl phosphate in *Escherichia coli* is sufficient for direct phosphorylation of two-component response regulators. J Bacteriol **189:**5574–5581. http://dx.doi.org/10.1128/JB.00564-07.
13. **Lukat GS, McCleary WR, Stock AM, Stock JB.** 1992. Phosphorylation of bacterial response regulator proteins by low molecular weight phosphodonors. Proc Natl Acad Sci U S A **89:**718–722. http://dx.doi.org/10.1073/pnas.89.2.718.
14. **Wolfe AJ, Chang DE, Walker JD, Seitz-Partridge JE, Vidaurri MD, Lange CF, Pruss BM, Henk MC, Larkin JC, Conway T.** 2003. Evidence that acetyl phosphate functions as a global signal during biofilm development. Mol Microbiol **48:**977–988. http://dx.doi.org/10.1046/j.1365-2958.2003.03457.x.
15. **Sadykov MR, Thomas VC, Marshall DD, Wenstrom CJ, Moormeier DE, Widhelm TJ, Nuxoll AS, Powers R, Bayles KW.** 2013. Inactivation of the Pta-AckA pathway causes cell death in *Staphylococcus aureus*. J Bacteriol **195:**3035–3044. http://dx.doi.org/10.1128/JB.00042-13.
16. **Ramos-Montanez S, Kazmierczak KM, Hentchel KL, Winkler ME.** 2010. Instability of *ackA* (acetate kinase) mutations and their effects on acetyl phosphate and ATP amounts in *Streptococcus pneumoniae* D39. J Bacteriol **192:**6390–6400. http://dx.doi.org/10.1128/JB.00995-10.
17. **Gueriri I, Bay S, Dubrac S, Cyncynatus C, Msadek T.** 2008. The Pta-AckA pathway controlling acetyl phosphate levels and the phosphorylation state of the DegU orphan response regulator both play a role in regulating *Listeria monocytogenes* motility and chemotaxis. Mol Microbiol **70:**1342–1357. http://dx.doi.org/10.1111/j.1365-2958.2008.06496.x.
18. **Zhao Y, Tomas CA, Rudolph FB, Papoutsakis ET, Bennett GN.** 2005. Intracellular butyryl phosphate and acetyl phosphate concentrations in *Clostridium acetobutylicum* and their implications for solvent formation. Appl Environ Microbiol **71:**530–537. http://dx.doi.org/10.1128/AEM.71.1.530-537.2005.
19. **Cramer A, Gerstmeir R, Schaffer S, Bott M, Eikmanns BJ.** 2006. Identification of RamA, a novel LuxR-type transcriptional regulator of genes involved in acetate metabolism of *Corynebacterium glutamicum*. J Bacteriol **188:**2554–2567. http://dx.doi.org/10.1128/JB.188.7.2554-2567.2006.
20. **Pruss BM, Verma K, Samanta P, Sule P, Kumar S, Wu J, Christianson D, Horne SM, Stafslien SJ, Wolfe AJ, Denton A.** 2010. Environmental and genetic factors that contribute to *Escherichia coli* K-12 biofilm formation. Arch Microbiol **192:**715–728. http://dx.doi.org/10.1007/s00203-010-0599-z.
21. **Kim JN, Ahn SJ, Seaton K, Garrett S, Burne RA.** 2012. Transcriptional organization and physiological contributions of the *relQ* operon of *Streptococcus mutans*. J Bacteriol **194:**1968–1978. http://dx.doi.org/10.1128/JB.00037-12.
22. **Terleckyj B, Willett NP, Shockman GD.** 1975. Growth of several cariogenic strains of oral streptococci in a chemically defined medium. Infect Immun **11:**649–655.
23. **Ahn SJ, Browngardt CM, Burne RA.** 2009. Changes in biochemical and phenotypic properties of *Streptococcus mutans* during growth with aeration. Appl Environ Microbiol **75:**2517–2527. http://dx.doi.org/10.1128/AEM.02367-08.
24. **Shubeita HE, Sambrook JF, McCormick AM.** 1987. Molecular cloning and analysis of functional cDNA and genomic clones encoding bovine cellular retinoic acid-binding protein. Proc Natl Acad Sci U S A **84:**5645–5649. http://dx.doi.org/10.1073/pnas.84.16.5645.
25. **Kremer BH, van der Kraan M, Crowley PJ, Hamilton IR, Brady LJ, Bleiweis AS.** 2001. Characterization of the sat operon in *Streptococcus mutans*: evidence for a role of Ffh in acid tolerance. J Bacteriol **183:**2543–2552. http://dx.doi.org/10.1128/JB.183.8.2543-2552.2001.
26. **Merritt J, Qi F, Shi W.** 2005. A unique nine-gene *comY* operon in *Streptococcus mutans*. Microbiology **151:**157–166. http://dx.doi.org/10.1099/mic.0.27554-0.
27. **LeBlanc DJ, Lee LN, Abu-Al-Jaibat A.** 1992. Molecular, genetic, and functional analysis of the basic replicon of pVA380-1, a plasmid of oral streptococcal origin. Plasmid **28:**130–145. http://dx.doi.org/10.1016/0147-619X(92)90044-B.
28. **Keating DH, Shulla A, Klein AH, Wolfe AJ.** 2008. Optimized two-dimensional thin layer chromatography to monitor the intracellular concentration of acetyl phosphate and other small phosphorylated molecules. Biol Proced Online **10:**36–46. http://dx.doi.org/10.1251/bpo141.
29. **Pericone CD, Park S, Imlay JA, Weiser JN.** 2003. Factors contributing to hydrogen peroxide resistance in *Streptococcus pneumoniae* include pyruvate oxidase (SpxB) and avoidance of the toxic effects of the Fenton reaction. J Bacteriol **185:**6815–6825. http://dx.doi.org/10.1128/JB.185.23.6815-6825.2003.
30. **Pruss BM, Wolfe AJ.** 1994. Regulation of acetyl phosphate synthesis and degradation, and the control of flagellar expression in *Escherichia coli*. Mol Microbiol **12:**973–984. http://dx.doi.org/10.1111/j.1365-2958.1994.tb01085.x.
31. **Lemos JA, Lin VK, Nascimento MM, Abranches J, Burne RA.** 2007. Three gene products govern (p)ppGpp production by *Streptococcus mutans*. Mol Microbiol **65:**1568–1581. http://dx.doi.org/10.1111/j.1365-2958.2007.05897.x.
32. **Abranches J, Candella MM, Wen ZT, Baker HV, Burne RA.** 2006. Different roles of EIIABMan and EIIGlc in regulation of energy metabolism, biofilm development, and competence in *Streptococcus mutans*. J Bacteriol **188:**3748–3756. http://dx.doi.org/10.1128/JB.00169-06.
33. **Lemos JA, Nascimento MM, Lin VK, Abranches J, Burne RA.** 2008. Global regulation by (p)ppGpp and CodY in *Streptococcus mutans*. J Bacteriol **190:**5291–5299. http://dx.doi.org/10.1128/JB.00288-08.
34. **Ahn SJ, Wen ZT, Brady LJ, Burne RA.** 2008. Characteristics of biofilm

formation by *Streptococcus mutans* in the presence of saliva. Infect Immun **76:**4259–4268. http://dx.doi.org/10.1128/IAI.00422-08.
35. **Loo CY, Corliss DA, Ganeshkumar N.** 2000. *Streptococcus gordonii* biofilm formation: identification of genes that code for biofilm phenotypes. J Bacteriol **182:**1374–1382. http://dx.doi.org/10.1128/JB.182.5.1374-1382.2000.
36. **Bochner BR, Ames BN.** 1982. Complete analysis of cellular nucleotides by two-dimensional thin layer chromatography. J Biol Chem **257:**9759–9769.
37. **Banas JA.** 2004. Virulence properties of *Streptococcus mutans*. Front Biosci **9:**1267–1277. http://dx.doi.org/10.2741/1305.
38. **Lemos JA, Burne RA.** 2008. A model of efficiency: stress tolerance by *Streptococcus mutans*. Microbiology **154:**3247–3255. http://dx.doi.org/10.1099/mic.0.2008/023770-0.
39. **Chang DE, Shin S, Rhee JS, Pan JG.** 1999. Acetate metabolism in a *pta* mutant of *Escherichia coli* W3110: importance of maintaining acetyl coenzyme A flux for growth and survival. J Bacteriol **181:**6656–6663.
40. **Brown TD, Jones-Mortimer MC, Kornberg HL.** 1977. The enzymic interconversion of acetate and acetyl-coenzyme A in *Escherichia coli*. J Gen Microbiol **102:**327–336. http://dx.doi.org/10.1099/00221287-102-2-327.
41. **Kajfasz JK, Rivera-Ramos I, Abranches J, Martinez AR, Rosalen PL, Derr AM, Quivey RG, Lemos JA.** 2010. Two Spx proteins modulate stress tolerance, survival, and virulence in *Streptococcus mutans*. J Bacteriol **192:**2546–2556. http://dx.doi.org/10.1128/JB.00028-10.
42. **Zhu L, Kreth J, Cross SE, Gimzewski JK, Shi W, Qi F.** 2006. Functional characterization of cell-wall-associated protein WapA in *Streptococcus mutans*. Microbiology **152:**2395–2404. http://dx.doi.org/10.1099/mic.0.28883-0.
43. **Wen ZT, Burne RA.** 2004. LuxS-mediated signaling in *Streptococcus mutans* is involved in regulation of acid and oxidative stress tolerance and biofilm formation. J Bacteriol **186:**2682–2691. http://dx.doi.org/10.1128/JB.186.9.2682-2691.2004.
44. **Higuchi M, Shimada M, Yamamoto Y, Hayashi T, Koga T, Kamio Y.** 1993. Identification of two distinct NADH oxidases corresponding to H_2O_2-forming oxidase and H_2O-forming oxidase induced in *Streptococcus mutans*. J Gen Microbiol **139:**2343–2351. http://dx.doi.org/10.1099/00221287-139-10-2343.
45. **Kreth J, Merritt J, Shi W, Qi F.** 2005. Competition and coexistence between *Streptococcus mutans* and *Streptococcus sanguinis* in the dental biofilm. J Bacteriol **187:**7193–7203. http://dx.doi.org/10.1128/JB.187.21.7193-7203.2005.
46. **Kai Y, Matsumura H, Izui K.** 2003. Phosphoenolpyruvate carboxylase: three-dimensional structure and molecular mechanisms. Arch Biochem Biophys **414:**170–179. http://dx.doi.org/10.1016/S0003-9861(03)00170-X.
47. **Sauer U, Eikmanns BJ.** 2005. The PEP-pyruvate-oxaloacetate node as the switch point for carbon flux distribution in bacteria. FEMS Microbiol Rev **29:**765–794. http://dx.doi.org/10.1016/j.femsre.2004.11.002.
48. **Morikawa M, Izui K, Taguchi M, Katsuki H.** 1980. Regulation of *Escherichia coli* phosphoenolpyruvate carboxylase by multiple effectors *in vivo*. Estimation of the activities in the cells grown on various compounds J Biochem **87:**441–449.
49. **Glenn K, Smith KS.** 2015. Allosteric regulation of *Lactobacillus plantarum* xylulose 5-phosphate/fructose 6-phosphate phosphoketolase (Xfp). J Bacteriol **197:**1157–1163. http://dx.doi.org/10.1128/JB.02380-14.
50. **Puri P, Goel A, Bochynska A, Poolman B.** 2014. Regulation of acetate kinase isozymes and its importance for mixed-acid fermentation in *Lactococcus lactis*. J Bacteriol **196:**1386–1393. http://dx.doi.org/10.1128/JB.01277-13.
51. **Chan SH, Norregaard L, Solem C, Jensen PR.** 2014. Acetate kinase isozymes confer robustness in acetate metabolism. PLoS One **9:**e92256. http://dx.doi.org/10.1371/journal.pone.0092256.
52. **Seaton K, Ahn SJ, Sagstetter AM, Burne RA.** 2011. A transcriptional regulator and ABC transporters link stress tolerance, (p)ppGpp, and genetic competence in *Streptococcus mutans*. J Bacteriol **193:**862–874. http://dx.doi.org/10.1128/JB.01257-10.
53. **Wen ZT, Nguyen AH, Bitoun JP, Abranches J, Baker HV, Burne RA.** 2011. Transcriptome analysis of LuxS-deficient *Streptococcus mutans* grown in biofilms. Mol Oral Microbiol **26:**2–18. http://dx.doi.org/10.1111/j.2041-1014.2010.00581.x.
54. **Pamp SJ, Frees D, Engelmann S, Hecker M, Ingmer H.** 2006. Spx is a global effector impacting stress tolerance and biofilm formation in *Staphylococcus aureus*. J Bacteriol **188:**4861–4870. http://dx.doi.org/10.1128/JB.00194-06.
55. **Ahn SJ, Wen ZT, Burne RA.** 2006. Multilevel control of competence development and stress tolerance in *Streptococcus mutans* UA159. Infect Immun **74:**1631–1642. http://dx.doi.org/10.1128/IAI.74.3.1631-1642.2006.